minerals

MDPI

Article

Mineralogy of Dolomite Carbonatites of Sevathur Complex, Tamil Nadu, India

Maria Rampilova [1,*], Anna Doroshkevich [1,2], Shrinivas Viladkar [3,4] and Elizaveta Zubakova [2,5]

1 Geological Institute, Siberian Branch of the Russian Academy of Sciences, Sakhyanova Street 6a, 670047 Ulan-Ude, Russia; doroshkevich@igm.nsc.ru
2 Sobolev Institute of Geology and Mineralogy, Siberian Branch of the Russian Academy of Sciences, Akademika Koptyuga Avenue 3, 630090 Novosibirsk, Russia; e.zubakova@g.nsu.ru
3 Indian Institute of Science Education and Research, Bhopal 462066, India; sviladkar@gmail.com
4 Carbonatite Research Centre, Amba Dongar, Kadipani 390117, India
5 Department of Geology and Geophysics, Novosibirsk State University, Pirogova Street 1, 630090 Novosibirsk, Russia
* Correspondence: mburtseva@mail.ru; Tel.: +7-951-637-0871

Abstract: The main mass of the Sevathur carbonatite complex (Tamil Nadu, India) consists of dolomite carbonatite with a small number of ankerite carbonatite dikes. Calcite carbonatite occurs in a very minor amount as thin veins within the dolomite carbonatite. The age ($^{207}Pb/^{204}Pb$) of the Sevathur carbonatites is 801 ± 11 Ma, they are emplaced within the Precambrian granulite terrains along NE–SW trending fault systems. Minor minerals in dolomite carbonatite are fluorapatite, phlogopite (with a kinoshitalite component), amphibole and magnetite. Pyrochlore (rich in UO_2), monazite-Ce, and barite are accessory minerals. Dolomite carbonatite at the Sevathur complex contains norsethite, calcioburbankite, and benstonite as inclusions in primary calcite and are interpreted as primary minerals. They are indicative of Na, Sr, Mg, Ba, and LREE enrichment in their parental carbonatitic magma. Norsethite, calcioburbankite, and benstonite have not been previously known at Sevathur. The hydrothermal processes at the Sevathur carbonatites lead to alteration of pyrochlore into hydropyrochlore, and Ba-enrichment. Also, it leads to formation of monazite-(Ce) and barite-II.

Keywords: dolomite carbonatites; pyrochlore; norsethite; benstonite; calcioburbankite; Sevathur; India

Citation: Rampilova, M.; Doroshkevich, A.; Viladkar, S.; Zubakova, E. Mineralogy of Dolomite Carbonatites of Sevathur Complex, Tamil Nadu, India. *Minerals* **2021**, *11*, 355. https://doi.org/10.3390/min11040355

Academic Editor: Davide Lenaz

Received: 23 February 2021
Accepted: 26 March 2021
Published: 29 March 2021

1. Introduction

Carbonatites are igneous rocks, which consist of more than 50 vol.% of primary magmatic carbonates and less than 20 wt.% of SiO_2 [1]. A wide range of deposits of strategically important mineral materials, such as rare (Nb, Ta, Zr, Li et al.), rare earth (REE+Y) and radioactive elements, as well as the apatite, and fluorite deposits and others, are associated with carbonatite complexes. A great scientific and practical interest in ore-bearing carbonatite complexes today has been caused by the accumulation of a considerable amount of information about their geological structure and mineral composition. Therefore, the study of carbonatite complexes, especially, mineralogy and ore formation processes, is important in fundamental science and in exploring the production process. In this paper, we present new mineralogical data on the Sevathur Nb-Ba-REE minerals because little information on many of these minerals is available in the literature, and also this will help to determine the history of crystallization and subsequent alteration of the Sevathur minerals.

The Sevathur carbonatite complex is the first discovered carbonatite from Tamil Nadu province in 1966 by the State Geology Survey [2] (also referred to as Koratti) and was confirmed by Deans in 1968 (Deans, unpublished report, Overseas Geological Survey, England). Earlier, the carbonatite was considered as banded limestone during prospecting for vermiculite deposits found within pyroxenite bordering carbonatite outcrop. In 1968, Semenov recognized pyrochlore from the Sevathur carbonatite, and Borodin delineated pyrochlore-rich zones in 1969. Afterward, detailed geological prospecting of the Sevathur

carbonatite and adjacent areas was carried out by the United Nations Development Program as part of the Tamil Nadu Mineral Development project. In later years, eight more carbonatite occurrences were reported from this region, all of which are located along the same NE-trending lineament [3], and intrusive into Archean Peninsular gneisses.

The Sevathur carbonatites contain high concentrations of apatite, monazite, magnetite, pyrochlore and vermiculite. The pyrochlore contains 24% of U_3O_8 [2] and occurred within early generation carbonatite, unlike most other carbonatite complexes in the Indian subcontinent. There are about 360 tons of Nb_2O and 1.2 million tons of vermiculite reserves in the Sevathur carbonatites [4].

In this paper, we present new data on the mineralogy of dolomite carbonatites of the Sevathur complex. Also, we discuss the post carbonatite emplacement hydrothermal processes those are responsible for the formation of some minerals.

2. Geological Setting

The Sevathur carbonatite complex is located near the same named village that is situated 9 km SSW of Tirupattur (Tamil Nadu, India). The age ($^{207}Pb/^{204}Pb$) of the Sevathur ankeritic carbonatites obtained by Schleicher et al. [5] is 801 $\pm$ 11 Ma. This age relates to the end of the carbonatitic magmatism because the ankeritic carbonatites are the youngest stage of carbonatite formation.

There are a large number of Proterozoic carbonatite complexes (Sevathur, Samalpatti, Jogipatti et al.) in southern India belonging to Precambrian (~1600–600 Ma) alkaline magmatism within the Eastern Ghats Mobile Belt (EGMB). They are emplaced within the Precambrian granulite terrains (Southern Ghats Terrain, SGT) along NE–SW trending fault systems [3,4,6].

In the Sevathur complex, dolomite carbonatite constitutes the main carbonatite exposure with a length of 2 km and an approximate width of 200 m in the central part (Figure 1).

The outcrop of the carbonatite is arcuate in form (strikes from N60°E–S60°W through to N–S to E–W) and shows an inward dip of about 60°. In addition to this major outcrop of carbonatite, there are few thin dikes of calcite and ankerite carbonatite; the largest being 400 m long and striking N5–E–S5–W. On the northern and western sides of the complex, the carbonatite is in contact with pyroxenite while at the southern end it is surrounded by granitic gneiss. Dolomite carbonatite shows presence of many xenoliths, which include protolith syenite, gneiss and pyroxenite. Magmatic banding is conspicuous in some parts of the outcrops. Along such banding sodic amphibole, sodic pyroxene, phlogopite, apatite, magnetite and pyrochlore are common minerals (Figure 2a).

In banded outcrops of carbonatite, some bands are particularly rich in magnetite, apatite and monazite (Figure 2b). Effects of fenitization upon the surrounding host rocks are widespread, such as the conversion of pyroxenite to vermiculite (in pyroxenite). "Contact fenite" formed at the immediate contact between carbonatite and peninsular gneiss contains aegirine- and orthoclase-rich zones while outcrops of syenite show incipient development of Na-pyroxene.

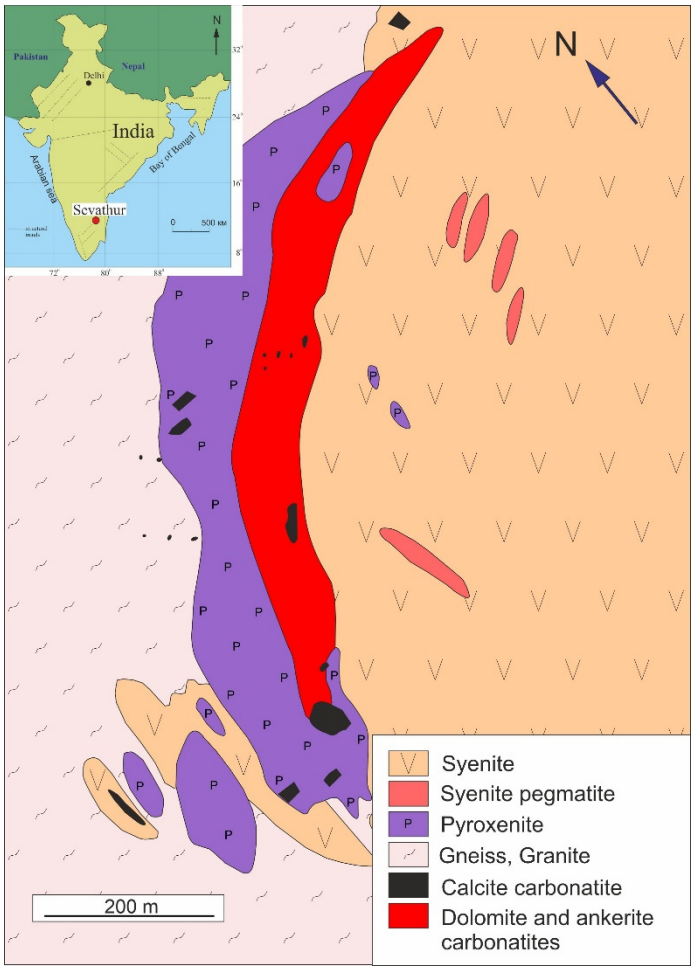

Figure 1. Geological scheme of the Sevathur carbonatitecomplex [4].

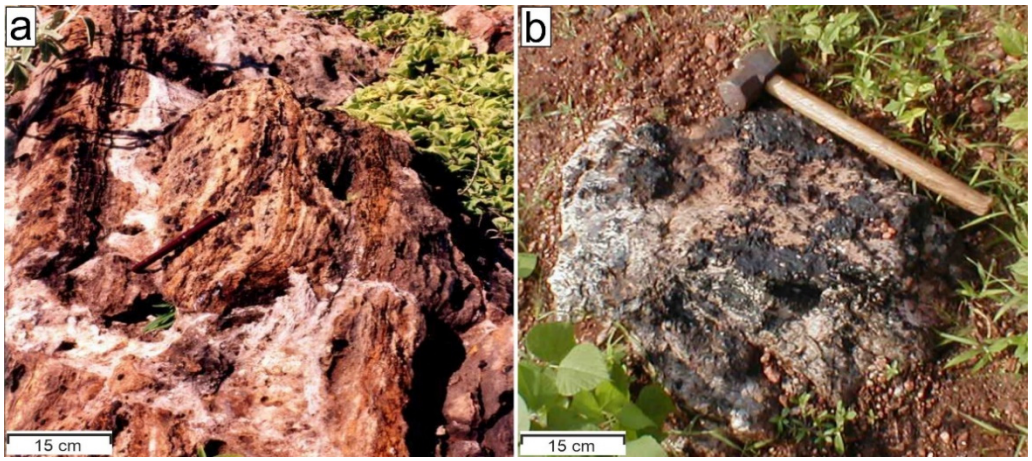

Figure 2. (**a**) Primary banding in the dolomite carbonatite outcrop at the Sevathur and (**b**) lumps rich in magnetite, pyrochlore and monazite.

3. Materials and Methods

Samples were collected from the central part of the massif during several field work explorations. Petrographic investigations of polished thin sections were carried out under a polarization microscope (OLYMPUS BX-51, OLYMPUS Co., Tokyo, Japan) in Geological Institute, Siberian Branch of the Russian Academy of Sciences (Ulan-Ude, Russia). Photos of photos of key moments are taken on a digital camera (MicroPublisher 3.3 RTV, Qlmaging,

Surrey, Canada). The rock textures and chemical compositions of the minerals were studied by polished rock samples under a scanning electron microscope with energy dispersive X-ray spectroscopy (LEO 1430VP EM, LEO Carl Zeiss SMT Ltd, Germany) with an Oxford Inca Energy 350 spectrometer, Oxford Instruments, Great Britain). The operation conditions for energy dispersive X-ray spectroscopy: 20 kV beam energy, 0.4 nA beam current, and 50 s spectrum live acquisition time. The results were tested against synthetic and natural minerals: SiO_2 (O,Si), BaF_2 (F,Ba), $NaAlSi_3O_8$ (Na), $MgCaSi_2O_6$ (Mg,Ca), Al_2O_3 (Al), $Ca_2P_2O_7$ (P), $KAlSi_3O_8$ (K), LaP_5O_{14} (La), CeP_5O_{14} (Ce), PrP_5O_{14} (Pr), NdP_5O_{14} (Nd), Cr met. (Cr), Mn met. (Mn) and Fe met. (Fe). Instrument error for REEs was less than 0.50 wt.%. Matrix correction was performed with the XPP algorithm as part of the built-in Inca Energy software. The polished rocks samples were analyzed at the Analytical center of mineralogical, geochemical and isotope Studies at the Geological Institute, Siberian Branch of the Russian Academy of Sciences (Ulan-Ude, Russia)

Chemical compositions of the minerals were also studied by electron microprobe (JEOL JXA-8100, JEOL Ltd., Japan). The operation conditions were: WDS mode, 20 kV, 15 nA, 1–2 μm beam diameter. For some minerals, we used a beam current of 10 nA and an acceleration voltage of 15 kV; for Fe–Ti oxides −20 nA and 15 kV; for monazite, −40 nA and 20 kV; and, for apatite, −10 nA and 20 kV. The peak counting time was 16 s for major and 30–60 s for minor elements. Natural minerals and synthetic phases were used as standards (element, detection limits in ppm): SiO_2 (Si, 158), rutile (Ti, 120), $LiNbO_3$ (Nb, 142), Sr silicate glass (Sr, 442), F-apatite (Ca, 115; P, 387; F, 477), hematite (Fe, 148), $CePO_4$ (Ce, 236), $LaPO_4$ (La, 272), $BaSO_4$ (S, 178), $NdPO_4$ (Nd, 362), Cl-apatite (Cl, 74), and $PrPO_4$ (Pr, 401). The electron microprobe studies were carried out at the Analytical Center for Multi-Elemental and Isotope Research Siberian Branch, Russian Academy of Science (Novosibirsk, Russia).

4. Results

The carbonatite outcrop mainly consists of dolomite carbonatite cut by a small number of ankerite carbonatite dikes. Calcite carbonatite are rare as thin veins cutting the dolomite carbonatite. The dolomite carbonatite has primarily medium- to coarse-grained structures and porphyritic textures. The porphyritic carbonatite contains phenocrysts of dolomite located within a matrix of equidimensional dolomite grains. There are laths of dolomite in such rocks. The dolomite carbonatites have rhythmic banding between medium- and fine-grained types. Banding is due to the presence of silicate minerals (for example, phlogopite, aegirine and Na-amphibole) along with magnetite, apatite, pyrochlore, monazite and zircon. In addition, there is leushite in the dolomite carbonatite [2]. Also, sulfides (pyrrhotite, pyrite, galena, and chalcopyrite) are present in accessory amounts. Pyrochlore is usually coarse-grained and occurs both as disseminated grains and in bands. It is enriched by UO_2 and is metamict [7].

The ankerite is usually unaltered in ankeritic carbonatite; however, some grains have undergone oxidation at the crystal margins or along the cleavage planes. Some phlogopite and amphibole grains are altered to chlorite. The contact between ankeritic carbonatite and the dolomitic one is prominent, with replacement of dolomitic carbonatite by later ankeritic fraction. Chlorite in contact zones is formed from amphibole andphlogopite. Such features are similar to the observed one along the contact between dolomitic and ankeritic carbonatites at Newania [8].

Dolomite ($CaMg(CO_3)_2$) (Figures 3 and 4) is the main carbonate mineral in all analyzed samples of dolomite carbonatite. It has low amounts of iron and manganese, and its content of strontium is less than in calcite (Table 1) (Figure 5).

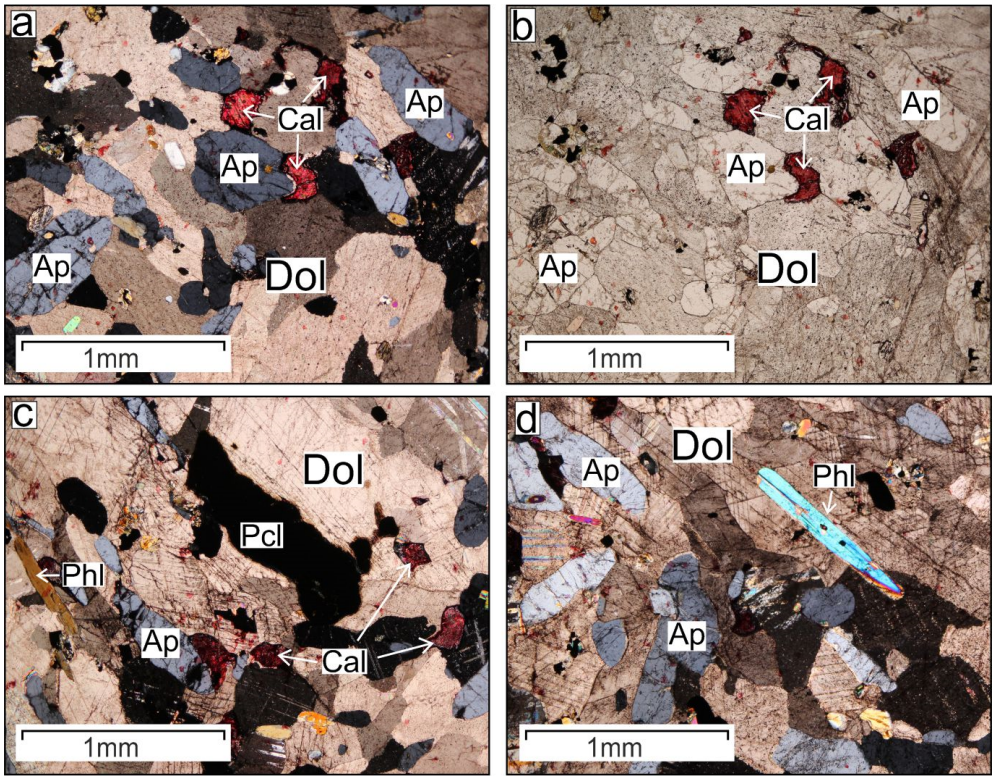

Figure 3. Thin section photomicrographs after staining with Alizarin Red showing micro-structures of the the Sevathur carbonatites. The red color denotes the presence of calcite. (**a**) (XPL view); (**b**) (PPL view) association of calcite (Cal), apatite (Ap) and dolomite (Dol); (**c**) association of calcite (Cal), apatite (Ap), phlogopite (Phl), pyrochlore (Pcl) and dolomite (Dol) (XPL view); and (**d**) association of apatite (Ap), phlogopite (Phl) and dolomite (Dol) (XPL view).

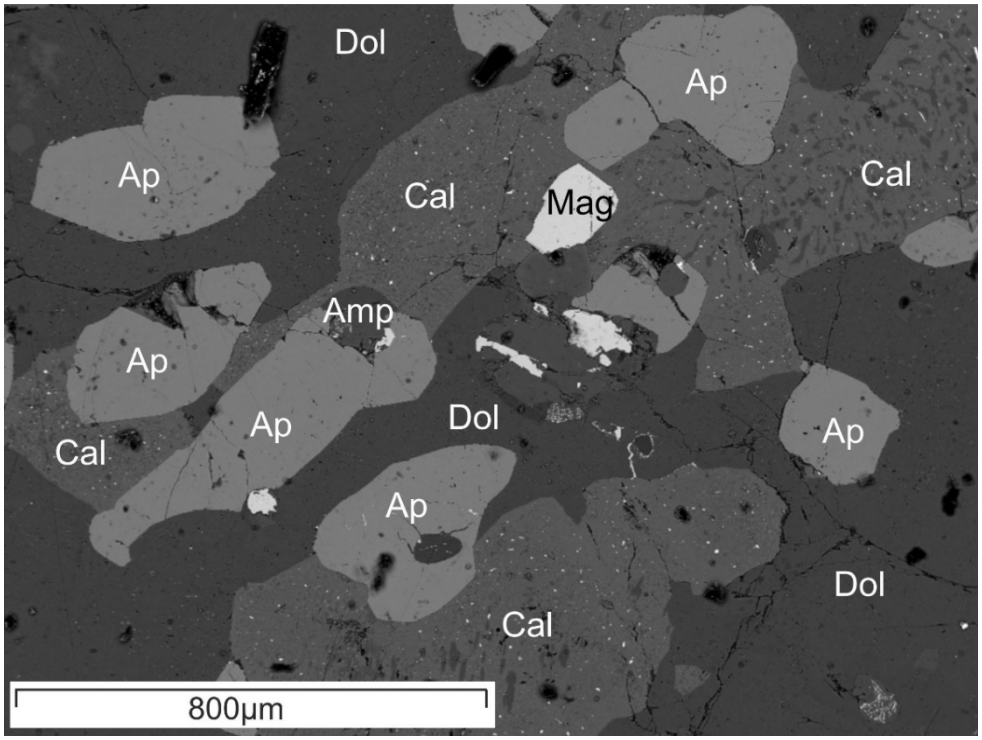

Figure 4. Association of calcite (Cal), apatite (Ap), magnetite (Mag), amphibole (Amp) and dolomite (Dol).

Table 1. Chemical composition of carbonate minerals from the Sevathur carbonatites, wt.%.

Component	**Dolomite**						**Calcite**						**Strontianite**					
FeO	4.48	3.95	4.40	3.94	3.87	3.33	0.45	0.53	0.93	0.71	0.96	1.31	b.d.	0.41	0.42	1.18	b.d.	b.d.
MnO	0.59	0.54	1.21	0.72	0.75	0.46	0.35	b.d.	b.d.	0.44	0.46	0.71	b.d.	b.d.	b.d.	b.d.	b.d.	b.d.
MgO	19.90	16.80	15.99	16.99	19.25	19.85	1.34	0.56	1.08	1.46	2.97	5.07	b.d.	b.d.	0.58	2.24	b.d.	b.d.
CaO	30.03	28.93	31.34	29.04	29.45	29.87	50.12	50.44	50.06	49.21	46.10	45.01	9.67	3.39	23.28	16.17	3.43	2.06
SrO	b.d.	1.12	1.13	1.22	b.d.	0.58	1.38	1.14	0.93	2.21	2.02	1.90	54.31	61.11	35.99	41.21	62.36	64.51
Na_2O	b.d.	b.d.	b.d.	b.d.	b.d.	b.d.	b.d.	b.d.	b.d.	b.d.	b.d.	b.d.	b.d.	b.d.	b.d.	b.d.	b.d.	b.d.
BaO	b.d.	b.d.	b.d.	b.d.	b.d.	b.d.	b.d.	0.51	b.d.	0.67	1.21	0.47	1.47	5.28	3.41	4.91	2.77	0.9
La_2O_3	b.d.	b.d.	b.d.	b.d.	b.d.	b.d.	b.d.	b.d.	b.d.	b.d.	b.d.	b.d.	b.d.	b.d.	b.d.	b.d.	b.d.	b.d.
Ce_2O_3	b.d.	b.d.	b.d.	b.d.	b.d.	b.d.	b.d.	b.d.	b.d.	b.d.	b.d.	b.d.	b.d.	b.d.	b.d.	b.d.	b.d.	b.d.
Pr_2O_3	b.d.	b.d.	b.d.	b.d.	b.d.	b.d.	b.d.	b.d.	b.d.	b.d.	b.d.	b.d.	b.d.	b.d.	b.d.	b.d.	b.d.	b.d.
Nd_2O_3	b.d.	b.d.	b.d.	b.d.	b.d.	b.d.	b.d.	b.d.	b.d.	b.d.	b.d.	b.d.	b.d.	b.d.	b.d.	b.d.	b.d.	b.d.
Total	55.00	51.35	54.07	51.91	53.33	54.10	53.64	53.18	53.00	54.70	53.73	54.48	65.45	70.18	63.68	65.72	68.56	67.47
Fe apfu	0.11	0.10	0.11	0.10	0.1	0.09	0.01	0.01	0.01	0.01	0.01	0.02	b.d.	0.01	0.01	0.02	b.d.	b.d.
Mn	0.02	0.02	0.03	0.02	0.02	0.01	0.01	b.d.	b.d.	0.01	0.01	0.01	b.d.	b.d.	b.d.	b.d.	b.d.	b.d.
Mg	0.90	0.89	0.85	0.89	0.90	0.91	0.04	0.02	0.03	0.04	0.08	0.13	b.d.	b.d.	0.02	0.07	b.d.	b.d.
Ca	0.97	0.97	0.99	0.97	0.98	0.98	0.93	0.96	0.95	0.91	0.87	0.82	0.24	0.09	0.51	0.37	0.09	0.06
Sr	b.d.	0.02	0.02	0.02	b.d.	0.01	0.01	0.01	0.01	0.02	0.02	0.02	0.75	0.85	0.43	0.5	0.88	0.93
Na	b.d.	b.d.	b.d.	b.d.	b.d.	b.d.	b.d.	b.d.	b.d.	b.d.	b.d.	b.d.	b.d.	b.d.	b.d.	b.d.	b.d.	b.d.
Ba	b.d.	b.d.	b.d.	b.d.	b.d.	b.d.	b.d.	b.d.	b.d.	0.01	0.01	b.d.	0.01	0.05	0.03	0.04	0.03	0.01
La	b.d.	b.d.	b.d.	b.d.	b.d.	b.d.	b.d.	b.d.	b.d.	b.d.	b.d.	b.d.	b.d.	b.d.	b.d.	b.d.	b.d.	b.d.
Ce	b.d.	b.d.	b.d.	b.d.	b.d.	b.d.	b.d.	b.d.	b.d.	b.d.	b.d.	b.d.	b.d.	b.d.	b.d.	b.d.	b.d.	b.d.
Pr	b.d.	b.d.	b.d.	b.d.	b.d.	b.d.	b.d.	b.d.	b.d.	b.d.	b.d.	b.d.	b.d.	b.d.	b.d.	b.d.	b.d.	b.d.
Nd	b.d.	b.d.	b.d.	b.d.	b.d.	b.d.	b.d.	b.d.	b.d.	b.d.	b.d.	b.d.	b.d.	b.d.	b.d.	b.d.	b.d.	b.d.
Component	**Norsethite**						**Barytocalcite**						**Benstonite**					
FeO	1.08	0.51	0.58	1.25	1.08	0.99	b.d.	b.d.	b.d.	b.d.	b.d.	b.d.	0.77	0.69	1.21	1.38	0.8	b.d.
MnO	b.d.	b.d.	b.d.	b.d.	b.d.	b.d.	b.d.	b.d.	b.d.	b.d.	b.d.	b.d.	b.d.	b.d.	b.d.	b.d.	b.d.	b.d.
MgO	16.55	13.71	13.96	14.01	12.55	15.19	2.92	2.16	b.d.	b.d.	0.8	2.52	10.51	12.39	9.57	13.35	2.67	1.74
CaO	1.4	1.64	4.04	1.9	2.74	6.63	20.75	19.6	24.68	16.83	20.95	21.27	12.98	8.27	18.79	9.4	19.48	23.52
SrO	b.d.	b.d.	0.91	0.6	0.66	0.88	1.54	2.81	0.78	6.75	2.24	4.06	0.93	b.d.	2.05	1.29	6.49	2.07
Na_2O	b.d.	b.d.	b.d.	b.d.	b.d.	b.d.	b.d.	b.d.	b.d.	b.d.	b.d.	b.d.	b.d.	b.d.	b.d.	b.d.	b.d.	b.d.
BaO	52.15	51.14	49.12	50.9	49.72	49.22	43.7	43.22	44.65	48.7	45.76	39.48	41.96	46.02	34.53	45.49	37.59	39.98
La_2O_3	b.d.	b.d.	b.d.	b.d.	b.d.	b.d.	b.d.	b.d.	b.d.	b.d.	b.d.	b.d.	b.d.	b.d.	b.d.	b.d.	b.d.	b.d.
Ce_2O_3	b.d.	b.d.	b.d.	b.d.	b.d.	b.d.	b.d.	b.d.	b.d.	b.d.	b.d.	b.d.	b.d.	b.d.	b.d.	b.d.	b.d.	b.d.
Pr_2O_3	b.d.	b.d.	b.d.	b.d.	b.d.	b.d.	b.d.	b.d.	b.d.	b.d.	b.d.	b.d.	b.d.	b.d.	b.d.	b.d.	b.d.	b.d.
Nd_2O_3	b.d.	b.d.	b.d.	b.d.	b.d.	b.d.	b.d.	b.d.	b.d.	b.d.	b.d.	b.d.	b.d.	b.d.	b.d.	b.d.	b.d.	b.d.
Total	71.18	67	68.61	68.67	66.76	72.9	68.91	67.79	70.11	72.29	70.09	67.33	67.16	67.37	66.15	70.91	67.03	67.54
Fe apfu	0.04	0.02	0.02	0.05	0.04	0.03	b.d.	b.d.	b.d.	b.d.	0.01	b.d.	0.18	0.16	0.28	0.31	0.19	b.d.
Mn	b.d.	b.d.	b.d.	b.d.	b.d.	b.d.	b.d.	b.d.	b.d.	b.d.	b.d.	b.d.	b.d.	b.d.	b.d.	b.d.	b.d.	b.d.
Mg	1.04	0.96	0.92	0.94	0.88	0.9	0.2	0.15	b.d.	b.d.	0.06	0.17	4.45	5.28	4.0	5.36	1.16	0.75
Ca	0.06	0.08	0.19	0.09	0.14	0.28	0.99	0.98	1.19	0.88	1.04	1.02	3.95	2.53	5.65	2.71	6.07	7.26
Sr	0	b.d.	0.02	0.02	0.02	0.02	0.04	0.08	0.02	0.19	0.06	0.11	0.15	b.d.	0.33	0.20	1.09	0.35
Na	b.d.	b.d.	b.d.	b.d.	b.d.	b.d.	b.d.	b.d.	b.d.	b.d.	b.d.	b.d.	b.d.	b.d.	b.d.	b.d.	b.d.	b.d.
Ba	0.86	0.94	0.85	0.9	0.92	0.77	0.77	0.79	0.79	0.93	0.83	0.7	4.67	5.16	3.80	4.80	4.29	4.51
La	b.d.	b.d.	b.d.	b.d.	b.d.	b.d.	b.d.	b.d.	b.d.	b.d.	b.d.	b.d.	b.d.	b.d.	b.d.	b.d.	b.d.	b.d.
Ce	b.d.	b.d.	b.d.	b.d.	b.d.	b.d.	b.d.	b.d.	b.d.	b.d.	b.d.	b.d.	b.d.	b.d.	b.d.	b.d.	b.d.	b.d.
Pr	b.d.	b.d.	b.d.	b.d.	b.d.	b.d.	b.d.	b.d.	b.d.	b.d.	b.d.	b.d.	b.d.	b.d.	b.d.	b.d.	b.d.	b.d.
Nd	b.d.	b.d.	b.d.	b.d.	b.d.	b.d.	b.d.	b.d.	b.d.	b.d.	b.d.	b.d.	b.d.	b.d.	b.d.	b.d.	b.d.	b.d.
Component	**Calcioburbankite**																	
FeO	b.d.	b.d.	b.d.	b.d.	b.d.	b.d.												
MnO	b.d.	b.d.	b.d.	b.d.	b.d.	b.d.												
MgO	b.d.	1.21	b.d.	b.d.	b.d.	b.d.												
CaO	16.45	16.51	15.63	8.1	9.21	15.08												
SrO	8.55	9.82	9.98	18.45	19.11	19.48												
Na_2O	3.33	3.95	5.00	10.18	9.44	3.09												
BaO	4.61	8.09	5.66	8.47	8.11	3.79												
La_2O_3	11.54	10.11	10.6	6.52	5.44	6.19												
Ce_2O_3	15.47	14.22	13.74	9.65	9.42	12.1												
Pr_2O_3	b.d.	1.56	1.23	b.d.	1.57	1.06												
Nd_2O_3	2.58	3.38	2.95	2.29	3.09	3.64												
Total	62.54	68.85	64.79	63.66	65.38	64.43												

Table 1. *Cont.*

Fe apfu	b.d.	b.d.	b.d.	b.d.	b.d.	b.d.
Mn	b.d.	b.d.	b.d.	b.d.	b.d.	b.d.
Mg	b.d.	b.d.	b.d.	b.d.	b.d.	b.d.
Ca	2.09	1.91	1.92	1.03	1.13	1.87
Sr	0.59	0.61	0.66	1.26	1.27	1.31
Na	0.76	0.83	1.11	2.33	2.10	0.69
Ba	0.21	0.34	0.25	0.39	0.37	0.17
La	0.50	0.40	0.45	0.28	0.23	0.26
Ce	0.67	0.56	0.58	0.42	0.40	0.51
Pr	b.d.	0.06	0.05	b.d.	0.07	0.04
Nd	0.11	0.13	0.12	0.10	0.13	0.15

Note. b.d.—below detection limit. Apfu—atom per formula units are based on 6 oxygens in dolomite, norsethite and barytocalcite; on 3 oxygens in calcite and strontianite; on 39 oxygens in benstonite and on 15 oxygens in calcioburbancite.

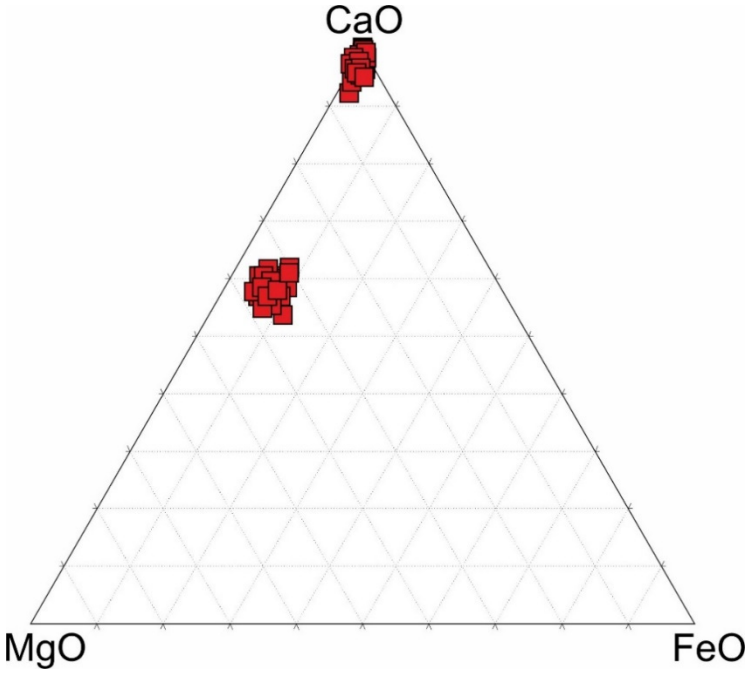

Figure 5. Composition of Sevathur carbonates in terms of CaO–MgO–FeO (wt. %).

Calcite ($CaCO_3$) formed later than dolomite and is interstitial between dolomite grains (Figures 3 and 4). It contains SrO, MgO and low amounts of FeO and MnO; sometimes it contains BaO (Table 1). Using the diagram of Goldsmith [9] we obtained that the subsolidus temperature of formation of calcite-dolomite is 600–650 °C. An average overall composition of the mixed carbonate was calculated by multiple spots on SEM/EDS (FeO 1.48–1.52, MnO 0.63–0.66, MgO 3.82–4.63, CaO 44.68–44.13, SrO 1.65–2.08).

Calcite contains exsolved dolomite (Figure 6). It also contains small inclusions of norsethite, baryte, strontianite, barytocalcite, benstonite and calcioburbankite (Figure 6).

Norsethite ($BaMg(CO_3)_2$) is found as small (up to 50 μm) exolutions within calcite (Figure 6b). It contains CaO and FeO, and in some cases SrO (Table 1).

Strontianite ($SrCO_3$) associates with barytocalcite (Figure 6). It contains CaO, BaO and sometimes MgO, FeO (Table 1).

Barytocalcite ($BaCa(CO_3)_2$) contains MgO and SrO (Table 1 and Figure 6).

Benstonite ($Ba_6Ca_6Mg(CO_3)_{13}$) forms small (up to 10 μm, Figure 6) inclusions within calcite. It is characterized by varying concentrations of BaO, CaO, MgO and SrO (Table 1). The benstonite compositional variation from Sevathur carbonatite can be expressed: $(Ba_{3.8–5.16}Sr_{0–1.09}Mg_{0–1.87})(Ca_{2.53–6}Mg_{0–3.47})(Mg_{0.54–1.78}Fe_{0–0.31})[CO_3]_{13}$. There are negative correlations between barium and calcium, calcium and magnesium, strontium and mag-

nesium (correlation coefficients −0.83, −0.71 and −0.72, respectively). Such values in Sevathur benstonite mean that there is a strong negative correlation between these elements, that is, if the concentrations of barium, calcium and strontium increase, then the concentrations of calcium, magnesium will decrease (Figure 7).

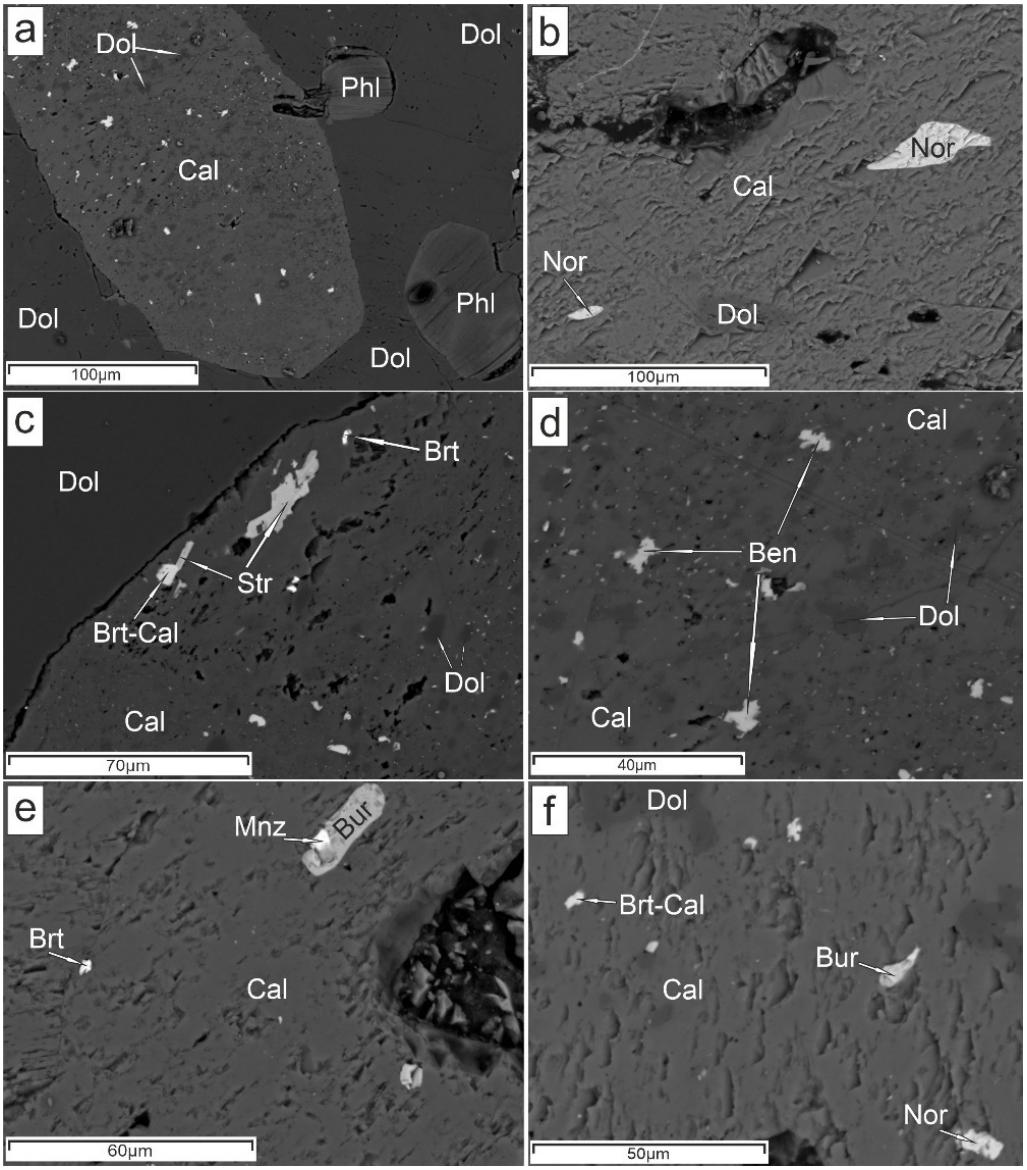

Figure 6. Back-scattered electron (BSE) images showing textural interrelations among inclusions of minerals and calcite in Sevathur carbonatites. (**a**) Primary calcite (Cal) and phlogopite (Phl) in dolomite (Dol) (note that inclusions of minerals are found exclusively in the core of the primary calcite). (**b**–**f**). Inclusions of norsethite (Nor), dolomite (Dol), baryte (Brt), strontianite (Str), barytocalcite (Brt-Cal), benstonite (Ben), calcioburbankite (Bur) and monazite (Mnz) in calcite (Cal).

Calcioburbankite ($Na_3(Ca,REE,Sr)_3(CO_3)_5$) forms small (up to 30 μm, Figure 6) inclusions within calcite and associates with monazite, benstonite, norsethite and baryte. It is characterized with varying concentrations of Na_2O, BaO, SrO, CaO, and TR_2O_3. The Sevathur calcioburbankite formulae can be expressed as: $(Na_{0.69–2.33}Ca_{0.67–2.09})(Sr_{0.59–1.31}LREE_{0.8–1.28}Ba_{0.17–0.39})[CO_3]_5$. A positive correlation between BaO and SrO; a negative correlation between TR_2O_3 and Na_2O, CaO + SrO + BaO and Na_2O+LREE are presented on Figure 8. The correlation coefficient of the Sevathur calcioburbankite is close to 1 (+0.68), then there is a positive correlation between BaO and SrO. The correlation coefficients between LREE

and Na_2O, CaO + SrO + BaO and Na_2O + LREE (−0.38 and −0.56 respectively) indicate a weak negative correlation between these variables and, also, a low dependence.

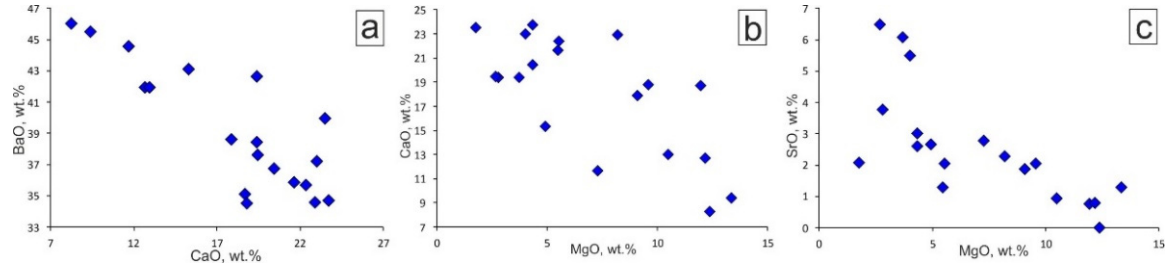

Figure 7. Plot of negative correlation between barium and calcium (**a**), calcium and magnesium (**b**), and strontium and magnesium (**c**), in benstonite.

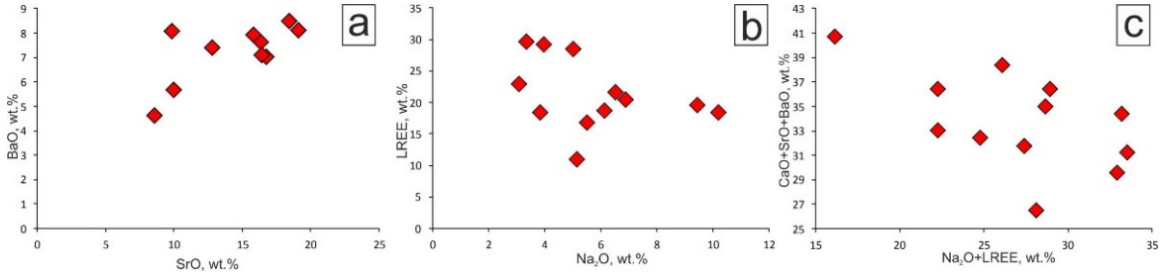

Figure 8. Plot of positive correlation between BaO and SrO (**a**); and a negative correlation between LREE and Na_2O (**b**), CaO + SrO + BaO and Na_2O + LREE (**c**) in calcioburbankite.

Baryte ($BaSO_4$) forms two generations. The first (baryte I) is presented by fine inclusions in calcite (Figure 6). The second generation (baryte II), forms rims and microcracks in calcite. The composition of these generations do not differ. It contains SrO (Table 2).

Table 2. Chemical composition of baryte from the Sevathur carbonatites, wt.%.

Component	3SE/5-3	SE6A/9	6SE-1/2	SE6A/4	6SE-1/16	3SE/7
CaO	1.56	b.d.	b.d.	3.13	4.24	1.25
BaO	62.00	62.44	65.06	58.80	56.41	64.83
SrO	3.00	2.20	1.20	4.42	5.12	0.67
SO_3	33.45	35.34	33.95	34.24	34.81	33.35
Total	100.01	99.98	100.21	100.59	100.58	100.10

Note. b.d.—below detection limit.

Fluorapatite ($Ca_5(PO_4)_3F$) forms prismatic crystals in dolomite (Figure 3, Figure 4, and Figure 9). There are inclusions of calcite, phlogopite and pyrochlore (Figure 9) in fluorapatite. It is enriched in strontium (Table 3).

Monazite-(Ce) ($CePO_4$) is embedded in calcite and dolomite, along with burbankite (Figure 6e). It also forms rims around apatite (Figure 9) and contains CaO (Table 3).

Amphibole ($Na(NaCa)Mg_5Si_8O_{22}(OH)_2$) is high magnesian (19.70–23.48 wt.% MgO) richterite with Na_2O (up to 5.88 wt.%) and CaO (6.18–9.02 wt.%) (Table 4). It forms single grains in dolomite and associates with apatite and magnetite (Figure 4).

Phlogopite ($KMg_3(AlSi_3O_{10})(OH)_2$) grains are enclosed in dolomite (Figure 3, Figure 6a and Figure 9c). It contains F, FeO and enriched in MgO (Table 5). Low concentration of K_2O in it is compensated by the kinoshitalite (up to 4.33 wt.% BaO) component (Table 5). Compositional variations of Si, Al, K and Ba indicate that the major exchange-reaction is Ba + Al ↔ K + Si. Structural formula is given in Table 5.

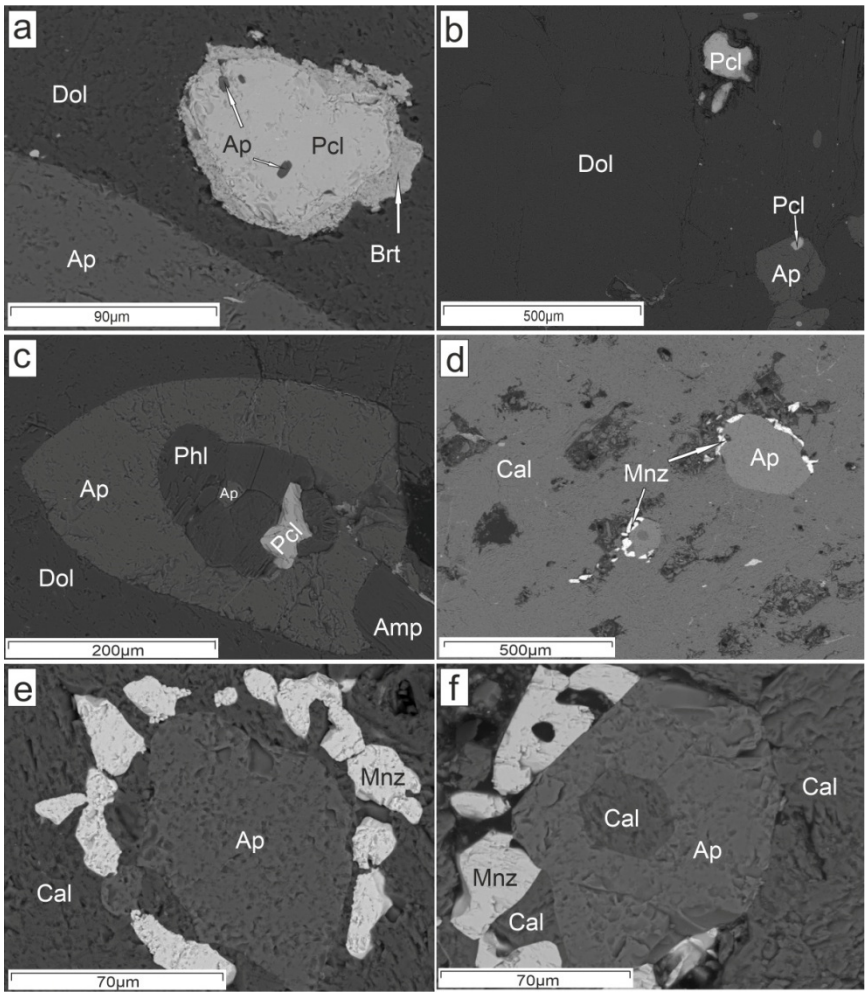

Figure 9. (**a**–**c**) Association of apatite (Ap), phlogopite (Phl) and pyrochlore (Pcl) in dolomite (Dol). (**d**–**f**) Monazite (Mnz) grains around apatite (Ap). Cal—calcite, Brt—baryte, Amp—amphibole.

Similar barium-rich micas are typical of some kimberlites [10] and also occurred in some carbonatite complexes, for example, in the Guli massif from the Maymecha–Kotuy province [11] and in the Chuktukon massif from the Chadobets upland in Russia [12], the Palabora Carbonatite Complex, South Africa [13] and in the metasomatized mantle xenoliths [14].

Magnetite ($Fe^{2+}Fe^{3+}{}_2O_4$) occurs in two generations (Figures 4 and 10). The first generation magnetite (magnetite I) occurs as isometric grains within calcite and dolomite. It is in solid solution with ilmenite (50.12–52.41 wt.%. TiO_2, 20.18–21.02 wt.%. MnO, 1.64–0.98 wt.%. MgO, 23.92–26.23 wt.%. FeO). It contains inclusions of amphibole, apatite and dolomite. Magnetite (II) of the second generation forms microveinlets in apatite and amphibole. However, the different generations of magnetite do not show a difference in their composition.

Pyrochlore is present in dolomite along with apatite, and it also sometimes contains inclusions of apatite (Figures 3 and 9). Pyrochlore is a hydropyrochlore $(H_2O,\square)_2Nb_2(O,OH)_6(H_2O)$ [15]. It has high concentrations of uranium and barium (Table 6).

Table 3. Chemical composition of fluorapatite and monazite-(Ce) from the Sevathur carbonatites, wt.%.

Component	Fluorapatite						Monazite-(Ce)					
SiO_2	0.035	0.127	0.016	0.003	0.008	0.024	b.d.	b.d.	b.d.	b.d.	b.d.	b.d.
FeO	0.127	0.278	0.147	0.233	0.009	0.027	b.d.	b.d.	b.d.	b.d.	b.d.	b.d.
MnO	0.078	0.038	0.053	0.067	0.029	0.056	b.d.	b.d.	b.d.	b.d.	b.d.	b.d.
CaO	53.658	53.502	53.969	53.770	53.730	53.495	1.900	2.070	0.700	1.410	0.280	0.580
Na_2O	0.254	0.280	0.243	0.192	0.217	0.224	b.d.	b.d.	b.d.	b.d.	b.d.	b.d.
SrO	1.533	1.442	1.372	1.481	1.595	1.424	b.d.	b.d.	b.d.	b.d.	b.d.	b.d.
MgO	0.061	0.016	0.056	0.065	0.011	0.016	b.d.	b.d.	b.d.	b.d.	b.d.	b.d.
P_2O_5	40.843	40.663	40.793	40.643	40.684	40.356	29.390	30.860	30.240	30.290	29.310	30.600
La_2O_3	0.203	0.247	0.204	0.187	0.242	0.220	19.470	19.490	20.830	23.560	23.160	21.770
Ce_2O_3	0.466	0.559	0.417	0.405	0.466	0.463	35.950	35.650	35.380	35.090	36.550	34.670
Pr_2O_3	0.004	0.048	0.083	0.056	0.046	0.050	1.760	3.350	2.150	1.950	2.320	2.430
Nd_2O_3	0.133	0.389	0.221	0.150	0.229	0.302	11.550	8.890	10.650	7.420	8.500	10.120
UO_2	0.045	b.d.	0.014	b.d.	b.d.	0.027	b.d.	b.d.	b.d.	b.d.	b.d.	b.d.
ThO_2	0.019	0.001	b.d.	0.011	0.037	0.030	b.d.	b.d.	b.d.	b.d.	b.d.	b.d.
SO_3	0.018	0.014	b.d.	0.003	b.d.	0.036	b.d.	b.d.	b.d.	b.d.	b.d.	b.d.
Cl	0.010	0.004	0.015	0.013	0.004	0.002	b.d.	b.d.	b.d.	b.d.	b.d.	b.d.
F	2.307	2.377	2.314	2.377	2.704	2.347	b.d.	b.d.	b.d.	b.d	b.d.	b.d.
Total	99.794	99.985	99.917	99.656	100.011	99.099	100.020	100.310	99.950	99.720	100.120	100.170
$F_2 = -O$	0.971	1.000	0.974	1.000	1.138	0.988	b.d.	b.d.	b.d.	b.d.	b.d.	b.d.
Si apfu	0.003	0.010	0.001	b.d.	0.001	0.001	b.d.	b.d.	b.d.	b.d.	b.d.	b.d.
Fe	0.008	0.018	0.009	0.015	0.001	0.002	b.d.	b.d.	b.d.	b.d.	b.d.	b.d.
Mn	0.005	0.002	0.003	0.004	0.002	0.004	b.d.	b.d.	b.d.	b.d.	b.d.	b.d.
Ca	4.315	4.307	4.338	4.337	4.335	4.341	0.080	0.080	0.030	0.060	0.010	0.020
Na	0.037	0.041	0.036	0.028	0.032	0.033	b.d.	b.d.	b.d.	b.d.	b.d.	b.d.
Sr	0.067	0.063	0.060	0.065	0.070	0.063	b.d.	b.d.	b.d.	b.d.	b.d.	b.d.
Mg	0.007	0.002	0.006	0.007	0.001	0.002	b.d.	b.d.	b.d.	b.d.	b.d.	b.d.
P	2.614	2.606	2.610	2.609	2.613	2.607	0.980	1.000	1.000	1.000	0.980	1.000
La	0.006	0.007	0.006	0.005	0.007	0.006	0.280	0.280	0.300	0.340	0.340	0.310
Ce	0.013	0.016	0.011	0.011	0.013	0.013	0.520	0.500	0.510	0.500	0.530	0.490
Pr	b.d.	0.001	0.002	0.002	0.001	0.001	0.030	0.050	0.030	0.030	0.030	0.030
Nd	0.004	0.011	0.006	0.004	0.006	0.008	0.160	0.120	0.150	0.100	0.120	0.140
U	0.001	b.d.	b.d.	b.d.	b.d.	0.001	b.d.	b.d.	b.d.	b.d.	b.d.	b.d.
Th	b.d.	b.d.	b.d.	b.d.	0.001	0.001	b.d.	b.d.	b.d.	b.d.	b.d.	b.d.
S	0.001	0.001	b.d.	b.d.	b.d.	0.002	b.d.	b.d.	b.d.	b.d.	b.d.	b.d.
Cl	0.001	0.001	0.002	0.002	0.001	b.d.	b.d.	b.d.	b.d.	b.d.	b.d.	b.d.
F	0.525	0.541	0.526	0.542	0.612	0.539	b.d.	b.d.	b.d.	b.d.	b.d.	b.d.

Note. b.d.—below detection limit, apfu—atom per formula units are based on 12 oxygens in apatite and on 4 oxygens in monazite-(Ce).

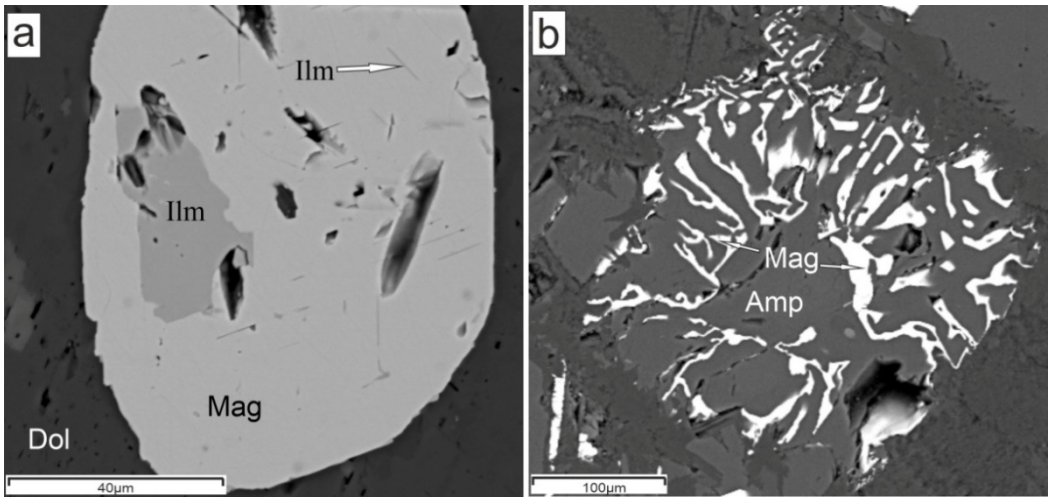

Figure 10. (**a**) Ilmenite (Ilm) in magnetite I (Mag) and (**b**) magnetite II in amphibole (Amp). Dolomite (Dol).

Table 4. Chemical composition of amphibole from the Sevathur carbonatites, wt.%.

Component	SE6A/1	SE6A/1-7	SE6A/3-2	SE6A/2-2	SE6A/3-8	6SE/13-7
SiO_2	56.01	57.19	56.69	57.16	56.74	57.51
Al_2O_3	0.89	0.77	0.94	0.79	1.13	1.23
FeO	5.8	4.85	4.84	4.98	5.38	3.99
MnO	0.00	0.54	0.49	0.45	0.5	0.36
MgO	23.46	23.05	23.23	22.97	22.27	23.48
CaO	6.18	6.35	6.67	6.63	6.76	9.02
Na_2O	5.88	5.73	5.65	5.16	5.14	3.64
K_2O	0.61	0.69	0.71	0.63	0.94	0.43
F	2.93	1.98	1.59	1.73	1.64	1.04
Total	101.76	101.15	100.81	100.50	100.5	100.7
$F_2 = -O$	1.23	0.83	0.67	0.73	0.69	0.44
Si apfu	7.75	7.81	7.75	7.82	7.78	7.77
Al	0.15	0.12	0.151	0.13	0.18	0.20
Fe^{3+}	0.00	0.31	0.30	0.31	0.34	0.25
Al	0.00	0.00	0.00	0.00	0.00	0.00
Mn	0.00	0.06	0.06	0.05	0.06	0.04
Fe^{2+}	0.67	0.25	0.25	0.26	0.28	0.21
Mg	4.84	4.69	4.73	4.68	4.56	4.73
Ca	0.92	0.93	0.98	0.97	0.99	1.31
Na	1.58	1.52	1.50	1.37	1.37	0.95
K	0.11	0.12	0.12	0.11	0.17	0.07
OH	0.72	1.15	1.31	1.25	1.29	1.56
F	1.28	0.86	0.69	0.75	0.71	0.44

Table 5. Chemical composition of phlogopite from the Sevathur carbonatites, wt.%.

Component	SE6A/1-1	SE6A/1-4	6SE/1-3	6SE/4	6SE/7	6SE/1-2
SiO_2	42.72	43.26	42.27	39.39	40.47	40.78
Al_2O_3	11.47	11.26	10.56	11.02	10.47	11.47
FeO	5.71	6.36	6.09	7.32	5.33	5.63
MgO	27.73	27.63	27.30	22.98	25.47	25.39
Na_2O	0.40	b.d.	0.77	b.d.	b.d.	b.d.
K_2O	9.46	10.37	9.75	8.93	9.32	9.37
BaO	1.40	b.d.	0.69	4.33	3.16	3.42
F	b.d.	2.31	2.09	b.d.	1.97	2.05
Total	98.89	101.19	99.52	93.97	96.19	98.11
$F_2 = -O$	b.d.	0.97	0.88	b.d.	0.83	0.86
Si apfu	2.96	2.98	2.93	2.97	2.99	2.96
Al	0.94	0.91	0.86	0.90	0.85	0.93
Fe	0.33	0.37	0.35	0.46	0.33	0.34
Mg	2.86	2.84	2.82	2.58	2.80	2.74
Na	0.05	0.00	0.10	b.d.	0.00	b.d.
K	0.84	0.91	0.86	0.86	0.88	0.87
Ba	0.04	b.d.	0.02	0.13	0.09	0.10
F	b.d.	0.50	0.47	b.d.	0.46	0.47

Note. b.d.—below detection limit, apfu—atom per formula units are based on 11 oxygens.

Table 6. Chemical composition of pyrochlore from the Sevathur carbonatites, wt.%.

Component	6SE/12-1	6SE/12-2	6SE/12-3	SE6A/3-2	SE6A/5-1	SE6A/7-2
Nb_2O_5	37.68	38.62	38.55	42.99	43.02	44.22
Ta_2O_5	4.66	3.54	2.71	5.14	6.13	6.84
SiO_2	3.04	1.45	2.31	b.d.	1.18	b.d.
TiO_2	4.47	4.52	6.54	5.00	4.19	5.77
UO_2	17.53	16.64	18.21	19.66	18.99	18.16
Al_2O_3	0.59	0.45	b.d.	b.d.	b.d.	b.d.

Table 6. *Cont.*

Component	6SE/12-1	6SE/12-2	6SE/12-3	SE6A/3-2	SE6A/5-1	SE6A/7-2
FeO	2.62	4.08	3.04	2.48	2.73	4.66
Ce_2O_3	1.32	1.63	3.63	b.d.	2.01	1.91
CaO	2.04	5.58	6.74	6.49	6.28	6.34
BaO	11.53	9.09	b.d.	8.20	5.66	7.37
SrO	1.94	3.94	2.74	2.77	2.59	4.13
PbO	b.d.	b.d.	2.38	1.82	2.48	2.08
Na_2O	b.d.	b.d.	b.d.	1.62	0.75	b.d.
Total	87.43	89.55	86.86	96.17	96.01	101.47
Ca apfu	0.15	0.43	0.50	0.50	0.47	0.44
Ba	0.32	0.25	b.d.	0.23	0.16	0.19
Sr	0.08	0.16	0.11	0.12	0.11	0.15
Na	0.00	0.00	0.00	0.23	0.10	b.d.
Ce	0.03	0.04	0.09	b.d.	0.05	0.04
U + Pb	0.27	0.26	0.32	0.36	0.35	0.30
Total A	0.85	1.14	1.02	1.44	1.24	1.12
Nb	1.2	1.24	1.2	1.41	1.36	1.28
Ta	0.09	0.07	0.05	0.10	0.12	0.12
Ti	0.30	0.30	0.42	0.34	0.28	0.35
Al	0.05	0.04	b.d.	b.d.	b.d.	b.d.
Fe	0.15	0.24	0.17	0.15	0.16	0.25
Si	0.21	0.10	0.16	b.d.	0.08	b.d.
Total B	2.00	1.99	2.00	2.00	2.00	2.00

Note. b.d.—below detection limit, apfu—atom per formula units are based on 2 B-site cations.

5. Discussion

5.1. Genesis of Ba-Mg-Sr-REE-Carbonates

Mineralogical and petrographical observations of the Sevathur dolomite carbonatites suggest the following paragenetic sequence (Figure 11).

The Sevathur carbonatites are enriched in Ba; it is reflected by their mineralogical composition. Mica with high Ba concentration and presence of independent Ba-minerals is evidenced.

Norsethite was reported for the first time in the sedimentary Green River Formation in Wyoming, USA [16]. It was also found in a carbonate body in metamorphosed braunite ores in Langban deposit, Sweden [17], in the Rosh Pinah hydrothermal zinc-lead deposit in Namibia [18], in skarns in Baita Bihor County, Romania [19], in iron-barite-sulfide ores in the Kremikovtsi deposit, Bulgaria [20], as well as in the carbonatite complexes in Vuoriyarvi, in the Kola peninsula, Russia [21,22], Chipman Lake, Ontario, Canada [23], and Tapira, SE Brazil [24].

Benstonite was discovered at a barium deposit in Hot Spring County, USA [25], and then was noted in skarns in Sweden [26] and USA [27], in a number of lead-zinc deposits in Scotland, Canada and Namibia [28], as well as in the Jogipatti carbonatites, India [29] and later described in detail by Vladykin et al. [30]. A special strontium variety of the benstonite was found in the Murun alkaline massif and at the Biraya ore occurrence [31,32].

The burbankite group consists of six mineral species: burbankite, khanneshite, calcioburbankite, remondite-(Ce), remondite-(La) and petersenite-(Ce). Burbankite is a widespread mineral, whereas other members of the group are rare. Belovitskaya and Pekov [33] identified three groups of chemical composition, corresponding to three genetic types of burbankite mineralization, which are associated with alkaline rocks. The first of them is related to carbonatites, the second one occurred in alkaline hydrothermalites and the third type is related to pectolite metasomatites of the Khibiny and the Murun massifs. In carbonatites the burbankite group minerals are rare with some exception and these are of early high temperature formation. Calcioburbankite, for the first time, was found in Mont Saint-Hilaire, Rouville County, Quebec, Canada [34]. In addition, it also occurs in carbonatite complexes of Vuoriyarvi [35], Srednaya Zima and Belaya Zima [36,37].

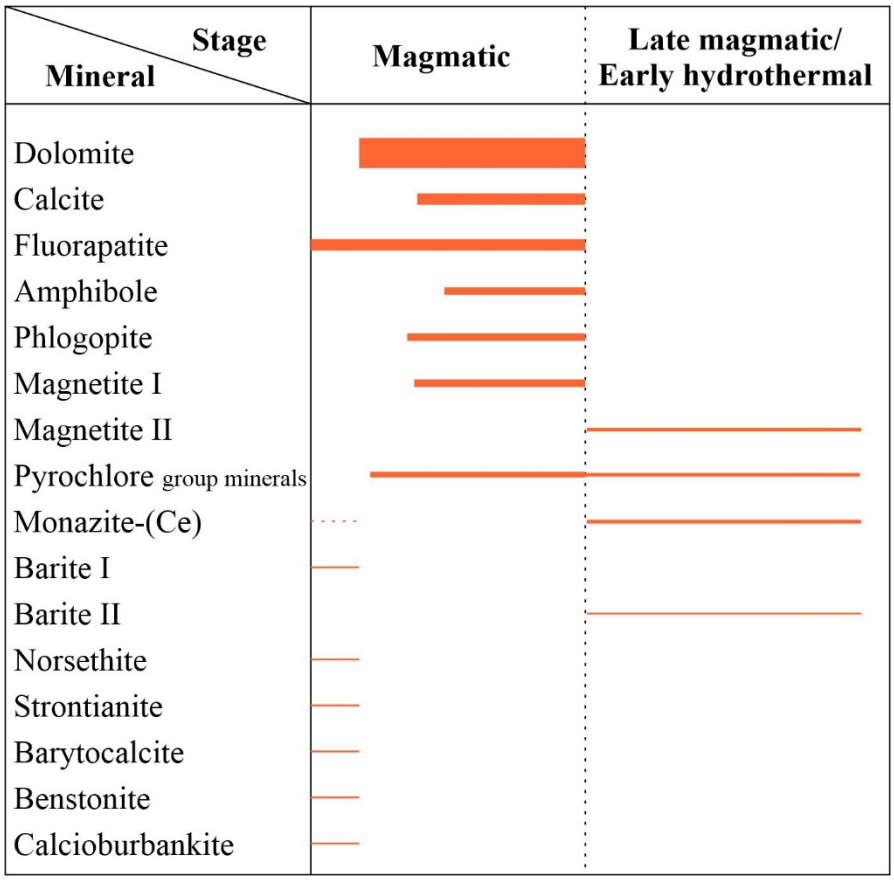

Figure 11. The proposed paragenetic sequence of minerals in the Sevathur carbonatites. Note: Line thickness indicates deposition intensity, the dotted line indicate possible mineral precipitation.

It is known that carbonatites contain high concentrations of Sr and Ba, and can contain up to 20 wt.% P_2O_5 at P > 20 kbar [38,39]. Although there are no low-P experimental data for Ba-, Sr- and phosphate-rich carbonatite melts, it is considered [40,41] on the basis of mineral inclusion investigations that primary burbankite-group phases, norsethite and bradleyite can also accompany dolomite or calcite in the natural environment.

Some intrusive carbonatites have poikilitic textures with relatively large (more than 0.6 mm across) grains of primary carbonate containing isometric crystals of calcite (in dolomite), dolomite (in calcite) and burbankite. Typical non-carbonate euhedral crystals, where present, include apatite, barite, monazite and fluorite. Some researchers [23,42,43] interpreted such mineral inclusions as either products of exsolution, or precipitates from a Na-rich immiscible fluid related with the initial carbonatitic melt. Chakhmouradian et al. [44,45] suggest such inclusions can be primary, and they are formed syngenetic with the parental mineral. Although apparently similar poikilitic intergrowths are produced by exsolution of initially homogeneous nonstoichiometric carbonate minerals during cooling, they can be identified due to their textural criteria. The round shape of mineral inclusions could be the argument of secondary origin [23], but is incomplete. For example, apatite is one of the earliest magmatic minerals in igneous carbonatites, and yet it usually occurs as isometric grains with no identifiable crystal forms [44].

Due to the limited miscibility between calcite and some other carbonate minerals at low T, early magmatic carbonates enriched in substituent elements can be expected to remain "unmix" upon cooling. However, the exsolution textures, formed by ionic diffusion in the solid state with no changes to the bulk composition of the grain, are rare. Chakhmouradian et al [44] described such cases including unmixed Ca-Ba-Sr "protocarbonates" and Mg-rich calcite. Other examples of intrusive carbonatites with exsolution textures: Calcite-dolomite intergrowths from Siilinjärvi in Finland, Kovdor in Russia and

Phalaborwa are shown in [46–48]; calcite-benstonite-barytocalcite(?) aggregates at Jogipatti, India, developed at the expense of Ca-Ba-Sr "protocarbonate", similar to that in the Murun Ba-Sr-carbonatites, but enriched in Mg [49].

Norsethite, barite I, strontianite, barytocalcite, benstonite and calcioburbankite were identified at the Sevathur carbonatite complex for the first time. These minerals form rare inclusions in magmatic calcite. We interpret the dolomite, norsethite, baryte, strontianite, barytocalcite, benstonite and calcioburbankite inclusions at Sevathur as primary because they are encapsulated in the core of calcite. It is assumed that they are formed as a result of the "protocarbonate" dissolution. The presence of these minerals implies enrichment of carbonatitic melt in Na, in addition to Sr, Ba and LREE.

5.2. Hydrothermal Alteration of U-Rich Pyrochlores

Pyrochlores from the Sevathur carbonatites show enrichment in Ba, Ta and U.

U is frequently concentrated in pyrochlore of worldwide carbonatites. Sometimes the concentration of UO_2 reaches significant values (e.g. U,Ti,Ta-pyrochlore from the Uganda carbonatized tuffs) [50]. The source of UO_2 in pyrochlore from the Sevathur carbonatites is primary because there is no secondary U-rich growth seen on any crystals of pyrochlore so far. In the majority of pyrochlore grains UO_2 is distributed all over the grains but sometimes U-rich areas are noticed in some grains. However, it is worth mentioning here that there are no U-minerals in the Sevathur carbonatites, even though these pyrochlore have undergone intense hydrothermal alteration and became metamict, thus their high concentration of UO_2 can be a source of U. Some researches [51] showed that the secondary processes are not affected on the content of U, Ta and Nb in pyrochlore.

It is well known that Ta is an important element in pyrochlore structure, for example [50–52]. For example, there is up to 27% Ta_2O_5 in uranopyrochlore from calcitic carbonatite of Siberia [52]. It is shown [53] that Nb-rich pyrochlore crystallizes at lower temperature than Ta-rich ones. The carbonatite magma was enriched in U and Ta, which became a part of pyrochlore. The Sevathur pyrochlore is one of the first crystallized minerals that formed simultaneously or a little later than apatite—it is confirmed by pyrochlore inclusions within apatite.

Sr and Ba are the common components of pyrochlore in worldwide carbonatites. For example, pyrochlore containing up to 0.2 apfu of Sr and Ba is presented in carbonatites from Chuktukon, Tomtor, Vuoriyarvi (Russia), Oka (Canada), Iron Hill (the USA) and Ashara (Brazil) [50]. Lapin and Kulikova, [54] advocated that Sr- and Ba-pyrochlore occur at the late stage of the carbonatite forming processes. However, some pyrochores enriched in Sr and Ba due to secondary ion exchange processes [55]. The low temperature hydrothermal alteration of pyrochlores leads to enrichment in Ba and Sr [56–59]. The hydrothermal processes at the Sevathur carbonatites lead to transformation of pyrochlore into hydropyrochlore, and also to their Ba-enrichment. In addition, hydrothermal processes led to formation of barite-II rims around pyrochlores.

An increased amount of Si of Sevathur pyrochlores is noteworthy. There are some points of view on silica position in pyrochlore structure. Some researches considered that silica occurs only as an impurity [60], or occurs in the radiation damaged structure of pyrochlore [61]. Other researchers suggest that Si can be included in the structure of the mineral during substitution reactions [62,63].

Based on investigation of pyrochlores from many sources, there are three stages of pyrochlore alteration: "primary" "transitional" and "secondary" [64]. There are two possible trends at the Sevathur pyrochlores: "transitional" and "secondary", while none of the pyrochlores plot in the "primary" alteration field [7]. These trends are determined by the contents of Ca, Fe, Sr, Ba, and Na. High temperature alteration is not found at the Sevathur pyrochlores, however, hydrothermal alteration is prominent.

Exchange reactions between primary pyrochlore and low-T hydrothermal fluids possibly occurred at relatively low pH, a_{Na}, a_{Ca2+} and high a_{HF}, a_{H2SO4}, a_{Sr} and a_{LREE}. These processes have been accompanied in element redistribution within the pyrochlore grains,

its enrichment in Sr, Ba, REE, Pb, and Si [63–65]. It is shown [64] that pyrochlore can undergo ion exchange and hydration at temperatures below 500 °C in acid or salt solutions.

5.3. Composition of Hydrothermal Fluids

Monazite-(Ce) occurs as rims around apatite grains. Similar monazites were found in the Khamambettu Carbonatites, Tamil Nadu, India [66], Central Aldan magnesiocarbonatites, Russia [67,68] and magnetite-apatite rocks of the Mushgai-Khudag Complex, South Mongolia [69]. The authors concluded that the monazite is the product of low-T hydrothermal processes of REE redistribution within the apatite.

Some experiments show [70–72] that monazite can form over a relatively wide range of temperatures (300–900 °C) and pressures (500–1000 MPa), but only in the presence of a fluid with a restricted range in composition [70–72]. These data suggest that fluid composition, but not pressure and temperature, is the main parameter facilitating (or suppressing) the formation of monazite during fluorapatite-fluid interaction. At the same time, it is determined [70–72] that H_2O is the principal agent, whether as a pure fluid or else mixed in some other substance such as CO_2 or KCl. Consequently, determining that precisely monazite is associated with REE-bearing fluorapatite helps to place constraints on the chemistry of the infiltrating fluids responsible both for the hydrothermal alteration of the fluorapatite as well as the rock as a whole [70–72]. Fluids responsible for REE transport and deposition have a high activity of ligands (F, Cl, CO_2(L), SO_4) and brines (for example, NaCl) [73–75].

There was no or was a little amount of Cl in hydrothermal fluids. It is confirmed by monazite composition. Broom-Fendley et al. [76] showed the absence of monazite during dissolution-reprecipitation of apatite, suggesting the presence of Cl-bearing fluids. Such a case was observed in the Tundulu and Kangankunde carbonatite complexes in the Chilwa Alkaline Province, Malawi [76]. Sulfur activity was low; it was absent either in apatite or in monazite. F was the main ligand. It is confirmed by composition of amphibole, phlogopite and apatite. The formation of monazite- (Ce) also indicates the mobility of F, Ca, and REE.

6. Conclusions

The presence of norsethite, barite, strontianite, barytocalcite, benstonite and calciobur-bankite inclusions in magmatic calcite implies enrichment of carbonatitic magma in Na, in addition to Sr, Ba and LREE. The phlogopite with kinoshitalite minal are consistent with the presence of Ba in carbonatite magma.

The hydrothermal fluid was enriched in F, P, REE, Ba and S, which led to the formation monazite-Ce, Ba-pyrochlore and barite II.

Author Contributions: Conceptualization, A.D., M.R. and S.V.; methodology, A.D., M.R. and S.V.; field research and provision of study materials, S.V.; data curation and validation, A.D., M.R. and S.V.; investigations, A.D., M.R. and E.Z.; writing—original draft, A.D. and M.R.; writing—review and editing, A.D., M.R. and S.V. All authors have read and agreed to the published version of the manuscript.

Funding: The investigations were supported by the Russian Science Foundation (RSF), project # 19-17-00019.

Data Availability Statement: Not applicable.

Acknowledgments: Analytical equipment for this study was provided by the Analytical Center for Multi-Elemental and Isotope Research Siberian Branch, Russian Academy of Science (Novosibirsk, Russia), "Analytical Center of Mineralogical, Geochemical and Isotope Studies" at the Geological Institute, Siberian Branch of the Russian Academy of Sciences (Ulan-Ude, Russia). The work was done on state assignment of IGM SB RAS (0330-2016-0002) and GIN SB RAS (AAAA-A21-121011390002-2).

Conflicts of Interest: The authors declare no conflict of interest.

References

1. Le Maitre, R.W.; Streckeisen, A.; Zanettin, B.; Le Bas, M.J.; Bonin, B.; Bateman, P.; Bellieni, G.; Dudek, A.; Efremova, S.; Keller, J.; et al. *Igneous Rocks: A Classification and Glossary of Terms. Recommendations of the International Union of Geological Sciences Subcommission on the Systematics of Igneous Rocks*, 2nd ed.; Le Maitre, R.W., Ed.; Cambridge University Press: Cambridge, UK, 2002; ISBN 9780521619486.
2. Borodin, L.S.; Gopal, V.; Moralev, V.M.; Subramanian, V. Precambrian carbonatites of Tamil Nadu, South India. *J. Geol. Soc. India* **1971**, *12*, 101–112.
3. Grady, J.C. Deep main faults in South India. *J. Geol. Soc. India* **1971**, *12*, 56–62.
4. Randive, K.; Meshram, T. An Overview of the carbonatites from the Indian subcontinent. *Open Geosci.* **2020**, *12*, 85–116. [CrossRef]
5. Schleicher, H.; Todt, W.; Viladkar, S.G.; Schmidt, F. Pb/Pb age determinations on Newania and Sevathur carbonatites of India: Evidence for multi-stage histories. *Chem. Geol.* **1997**, *140*, 261–273. [CrossRef]
6. Viladkar, S.G.; Subramanian, V. Mineralogy and geochemistry of the carbonatites of the Sevathur and Samalpatti complexes, Tamil Nadu. *J. Geol. Soc. India* **1995**, *45*, 505–517.
7. Viladkar, S.G.; Bismayer, U. U-rich pyrochlore from Sevathur carbonatites, Tamil Nadu. *J. Geol. Soc. India* **2014**, *83*, 147–154. [CrossRef]
8. Viladkar, S.G.; Wimmenauer, W. Mineralogy and geochemistry of the Newania carbonatite-fenite complex, Rajasthan, India. *N. Jb. Miner. Abh.* **1986**, *156*, 1–21.
9. Goldsmith, J.R.; Graf, D.L.; Witters, J.; Northrop, D.A. Studies in the synthetic $CaCO_3$-$MgCO_3$-$FeCO_3$: 1. Phase relations; 2. A method for major-element spectrochemical analysis; 3. Compositions of some ferrian dolomites. *J. Geol.* **1962**, *70*, 659–688. [CrossRef]
10. Mitchell, R.H. *Kimberlite, Orangeites and Related Rocks*; Plenum Press: New York, NY, USA, 1995; 410p.
11. Kogarko, L.N.; Ryabchikov, I.D.; Kuzmin, D.V. High-Ba mica in olivinites of the Guli massif (Maymecha–Kotuy province, Siberia). *Russ. Geol. Geophys.* **2012**, *53*, 1209–1215. [CrossRef]
12. Doroshkevich, A.G.; Chebotarev, D.A.; Sharygin, V.V.; Prokopyev, I.R.; Nikolenko, A.M. Petrology of alkaline silicate rocks and carbonatites of the Chuktukon massif, Chadobets upland, Russia: Sources, evolution and relation to the Triassic Siberian LIP. *Lithos* **2019**, *332–333*, 245–260. [CrossRef]
13. Giebel, R.J.; Marks, M.A.W.; Gauert, C.D.K.; Markl, G. A model for the formation of carbonatite-phoscorite assemblages based on the compositional variations of mica and apatite from the Palabora Carbonatite Complex, South Africa. *Lithos* **2019**, *324–325*, 89–104. [CrossRef]
14. Kogarko, L.N.; Kurat, G.; Ntaflos, T. Henrymeyerite in the metasomatized upper mantle of eastern Antarctica. *Can. Mineral.* **2007**, *45*, 497–501. [CrossRef]
15. Atencio, D.; Andrade, M.B.; Christy, A.G.; Giere, R.; Kartashov, P.M. The pyrochlore supergroup of minerals: Nomenclature. *Can. Mineral.* **2010**, *48*, 673–698. [CrossRef]
16. Mrose, M.E.; Chao, E.C.T.; Fahey, J.J.; Milton, C. Norsethite, $BaMg(CO_3)_2$, a new mineral from the Green River formation, Wyoming. *Am. Mineral.* **1961**, *46*, 420–429.
17. Sundius, N.; Blix, R. Norsethite from Lengban. *Arkiv. Mineral. Geol.* **1965**, *4*, 277–278.
18. Steyn, J.G.D.; Watson, M.D. Note on a new occurrence of norsethite, $BaMg(CO_3)_2$. *Amer. Miner.* **1967**, *52*, 1770–1775.
19. Onac, B.P. Caves formed within Upper Cretaceous skarns at Baita, Bihor County, Romania: Mineral deposition and speleogenesis. *Can. Miner.* **2002**, *40*, 1693–1703. [CrossRef]
20. Zidarov, N.; Petrov, O.; Tarassov, M.; Damyanov, Z.; Tarassova, E.; Petkova, V.; Kalvachev, Y.; Zlatev, Z. Mn-rich norsethite from the Kremikovtsi ore deposit, Bulgaria. *N. Jb. Miner. Abh.* **2009**, *186*, 321–331.
21. Kapustin, J.L. Norsethite—The first find in USSR. *Doklady Acad. Nauk USSR* **1965**, *161*, 922–924. (In Russian)
22. Kozlov, E.; Fomina, E.; Sidorov, M.; Shilovskikh, V.; Bocharov, V.; Chernyavsky, A.; Huber, M. The petyayan-vara carbonatite-hosted rare earth deposit (Vuoriyarvi, NW Russia): Mineralogy and geochemistry. *Minerals* **2020**, *10*, 73. [CrossRef]
23. Platt, R.G.; Woolley, A.R. The carbonatites and fenites of Chipman lake, Ontario. *Can. Miner.* **1990**, *28*, 241–250.
24. Secco, L.; Lavina, L. Crystal chemistry of two natural magmatic norsethites, $BaMg(CO_3)_2$, from an Mg-carbonatites of the alkaline carbonatitic complex of Tapira (SE Brazil). *N. Jb. Miner. Mh.* **1999**, *2*, 87–96.
25. Lippman, F. Benstonite, $Ca_7Ba_6(CO_3)_{l3}$, a new mineral from barite deposits in Hot Spring County, Arkansas. *Amer. Miner.* **1962**, *47*, 585–598.
26. Sundius, N. Benstonite and tephroite from Longban. *Ark. Miner. Geol.* **1963**, *3*, 407–411.
27. White, J.S., Jr.; Jarosewich, E. Second occurrence of benstonite. *Miner. Rec.* **1970**, *1*, 140–141.
28. Finlow-Bates, T. The possible significance of uncommon barium-rich mineral assemlages in sediment-hosted lead-zinc deposits. *Geol. Mijnbouw.* **1987**, *66*, 65–66.
29. Semenov, E.; Gopal, V.; Subramaian, V. Note on the occurrence of benstonite. *Surr. Sci.* **1971**, *40*, 62–67.
30. Vladykin, N.V.; Viladkar, S.G.; Miyazaki, T.; Mohan, R.V. Geochemistry of benstonite and associated carbonatites of Sevathur, Jogipatti and Samalpatti, Tamil Nadu, South India and Murun massif, Siberia. *J. Geol. Soc. India* **2008**, *72*, 312–324.
31. Ontoyev, D.O.; Dmitrieva, M.T.; Ontoeva, T.D. About strontium variety of benstonite. *Zap. Ross. Mineral. O-va* **1986**, *4*, 496–501.
32. Konev, A.A.; Kartashev, P.M.; Koneva, A.A.; Ushchapovskaya, Z.F.; Nartova, N.V. Mg-deficient strontium benstonite from the ore occurrence Biraya (Siberia). *Zap. Ross. Mineral. O-va* **2004**, *133*, 65–73.

33. Belovitskaya, Y.V.; Pekov, I.V. Genetic mineralogy of the burbankite group. *New Data Miner.* **2004**, *39*, 50–64.
34. Van Velthuizen, J.; Gault, R.; Grice, J.D. Calcioburbankite, $Na_3(Ca,REE,Sr)_3(CO_3)_5$, a new mineral species from Mont Saint Hilaire, Quebec, and its relationship to the burbankite group of minerals. *Can. Mineral.* **1995**, *33*, 1231–1235.
35. Subbotin, V.V.; Voloshin, A.V.; Pakhomovskii, Y.A.; Bakhchisaraitsev, A.Y. Calcioburbankite and burbankite from Vuoriyarvi carbonatite massif (new data). *Zap. Ross. Mineral. O-va* **1999**, *1*, 78–87. (In Russian)
36. Pozharitskaya, L.K.; Samoilov, V.S. *Petrology, Mineralogy and Geochemistry of Carbonatites of East Siberia (Petrologiya, Mineralogiyai Geokhimiya Karbonatitov Vostochnoi Sibiri)*; Nauka: Moscow, Russia, 1972; 268p. (In Russian)
37. Khromova, E.A. *Age and Petrogenesis of Rocks of the Alkaline-Ultrabasic Carbonatite Belaya Zima Massif (Eastern Sayan)*; Candidate of Geology, Geological Institute Siberian Branch of the Russian Academy of Sciences: Ulan-Ude, Russia, 2020. (In Russian)
38. Baker, M.B.; Wyllie, P.J. High-pressure apatite solubility in carbonate-rich liquids: Implications for mantle metasomatism. *Geochim. Cosmochim. Acta* **1992**, *56*, 3409–3422. [CrossRef]
39. Ryabchikov, I.D.; Hamilton, D.L. Interaction of carbonate-phosphate melts with mantle peridotites at 20–35 kbar. *S. Afr. J. Geol.* **1993**, *96*, 143–148.
40. Zaitsev, A.N.; Chakhmouradian, A.R. Calcite-amphiboleclinopyroxene rock from the Afrikanda complex, Kola Peninsula, Russia: Mineralogy and a possible link to carbonatites. II Oxysalt minerals. *Can. Mineral.* **2002**, *40*, 103–120. [CrossRef]
41. Zaitsev, A.N.; Sitnikova, M.A.; Subbotin, V.V.; Fernández-Suárez, J.; Jeffries, T.E. Sallanlatvi complex—A rare example of magnesite and siderite carbonatites. In *Phoscorites and Carbonatites from Mantle to Mine*; Wall, F., Zaitsev, A.N., Eds.; Mineralogical Society of Great Britain and Ireland: London, UK, 2004; pp. 201–245.
42. Faiziev, A.R.; Iskandarov, F.S.; Gafurov, F.G. Mineralogical and petrogenetic characteristics of carbonatites of Dunkeldykskii alkali massif (eastern Pamirs). *Proc. Russ. Mineral. Soc.* **1998**, *127*, 54–57. (In Russian)
43. Tichomirowa, M.; Whitehouse, M.J.; Gerdes, A.; Götze, J.; Schulz, B.; Belyatsky, B.V. Different zircon recrystallization types in carbonatites caused by magma mixing: Evidence from U–Pb dating, trace element and isotope composition (Hf and O) of zircons from two Precambrian carbonatites from Fennoscandia. *Chem. Geol.* **2013**, *353*, 173–198. [CrossRef]
44. Chakhmouradian, A.R.; Reguir, E.P.; Zaitsev, A.N. Calcite and dolomite in intrusive carbonatites. I. Textural variations. *Mineral. Petrol.* **2016**, *110*, 333–360. [CrossRef]
45. Chakhmouradian, A.R.; Dahlgren, S. Primary inclusions of burbankite in carbonatites from the Fen complex, southern Norway. *Miner. Petrol.* **2021**, *115*, 161–171. [CrossRef]
46. Puustinen, K. Dolomite exsolution textures in calcite from the Siilinjärvi carbonatite complex, Finland. *Bull. Geol. Soc. Finl.* **1974**, *46*, 151–159. [CrossRef]
47. Zaitsev, A.N.; Polezhaeva, L. Dolomite-calcite textures in early carbonatites of the Kovdor ore deposit, Kola peninsula, Russia: Their genesis and application for calcite-dolomite geothermometry. *Contrib. Mineral. Petrol.* **1994**, *115*, 339–344. [CrossRef]
48. Dawson, J.B.; Hinton, R.W. Trace-element content and partitioning in calcite, dolomite and apatite in carbonatite, Phalaborwa, South Africa. *Min. Mag.* **2003**, *67*, 921–930. [CrossRef]
49. Konev, A.A.; Vorob'ev, E.I.; Lazebnik, K.A. *Mineralogy of the Murun Alkaline Massif*; Siberian Branch Russian Academy of Sciences: Novosibirsk, Russia, 1996; p. 221. (In Russian)
50. Yaroshevsky, A.A.; Bagdasarov, Y.A. Geochemical diversity of minerals of the pyrochlore group. *Geochem. Int.* **2008**, *46*, 1245–1266. [CrossRef]
51. Redkin, A.F.; Borodulin, G.P. Pyrochlores as indicators of the uranium bearing potential of magmatic melts. *Dokl. Earth Sci.* **2010**, *432*, 787–790. [CrossRef]
52. Hogarth, D.D. Pyrochlore, apatite and amphibole: Distinctive minerals in carbonatite. In *Carbonatites: Genesis and Evolution*; Bell, K., Ed.; Unwin Hyman: London, UK, 1989; pp. 105–148.
53. Kjarsgaard, K.J.; Mitchell, R.H. Solubility of Ta in the system $CaCO_3$–$Ca(OH)_2$–$NaTaO_3$– $NaNbO_3$ ± F at 0.1 GPa: Implications for the crystallization of pyrochlore-group minerals in carbonatites. *Can. Mineral.* **2008**, *46*, 981–990. [CrossRef]
54. Lapin, A.V.; Kulikova, I.M. Alteration processes in pyrochlore and their products in weathering crusts of carbonatites. *Zap. Ross. Mineral. O-va* **1989**, *118*, 41–49.
55. Entin, A.R.; Yeremenko, G.Y.; Tyan, O.A. Stages of alteration of primary pyrochlores. *Trans. (Dokaldy) U.S.S.R. Acad. Sci. Earth Sci. Sect.* **1993**, *320*, 236–239.
56. Jager, E.; Niggli, E.; Van Der Veen, A.H. A hydrated bariumstrontium pyrochlore in a biotite rock from Panda Hill, Tanganyika. *Mineral. Mag.* **1959**, *32*, 10–25.
57. Van Wambeke, L. Pandaite, baddeleyite and associated minerals from the Bingo niobium deposit, Kivu, Democratic Republic of Congo. *Miner. Depos.* **1971**, *6*, 153–155. [CrossRef]
58. Van Wambeke, L. Kalipyrochlore, a new mineral of the pyrochlore group. *Am. Mineral.* **1978**, *63*, 528–530.
59. Hogarth, D.D.; Williams, C.T.; Jones, P. Primary zoning in pyrochlore group of minerals from carbonatites. *Mineral. Mag.* **2000**, *64*, 683–697. [CrossRef]
60. Hogarth, D. The pyrochlore group. *Am. Mineral.* **1977**, *62*, 403–410.
61. Bonazzi, P.; Bindi, L.; Zoppi, M.; Capitani, G.C.; Olmi, F. Single-crystal diffraction and transmission electron microscopy studies of "silicified" pyrochlore from Narssarssuk, Julianehaab district, Greenland. *Am. Mineral.* **2006**, *91*, 794–801. [CrossRef]
62. Williams, C.T.; Wall, F.; Woolley, A.R.; Phillipo, S. Compositional variation in pyrochlore from the Bingo carbonatite, Zaire. *J. Afr. Earth Sci.* **1997**, *25*, 137–145. [CrossRef]

63. Nasraoui, M.; Bilal, E. Pyrochlores from the Lueshe carbonatite complex (Democratic Republic of Congo): A geochemical record of deferent alteration stages. *J. Asian Earth Sci.* **2000**, *18*, 237–251. [CrossRef]
64. Lumpkin, G.R.; Ewing, R.C. Geochemical alteration of pyrochlore group minerals: Pyrochlore subgroup. *Am. Mineral.* **1995**, *80*, 732–742. [CrossRef]
65. Chebotarev, D.A.; Doroshkevich, A.G.; Klemd, R.; Karmanov, N.S. Evolution of Nb-mineralization in the Chuktukon carbonatite massif, Chadobets upland (Krasnoyarsk Territory, Russia). *Period. Mineral.* **2017**, *86*, 99–118.
66. Burtseva, M.V.; Ripp, G.S.; Doroshkevich, A.G.; Viladkar, S.G.; Rammohan, V. Features of mineral and chemical composition of the Khamambettu carbonatites, Tamil Nadu. *J. Geol. Soc. India* **2013**, *81*, 655–664. [CrossRef]
67. Prokopyev, I.R.; Doroshkevich, A.G.; Ponomarchuk, A.V.; Sergeev, S.A. Mineralogy, age and genesis of apatite-dolomite ores at the Seligdar apatite deposit (Central Aldan, Russia). *Ore Geol. Rev.* **2017**, *81*, 296–308. [CrossRef]
68. Prokopyev, I.R.; Doroshkevich, A.G.; Sergeev, S.A.; Ernst, R.E.; Ponomarev, J.D.; Redina, A.A.; Chebotarev, D.A.; Nikolenko, A.M.; Dultsev, V.F.; Moroz, T.N.; et al. Petrography, mineralogy and SIMS U-Pb geochronology of 1.9–1.8 Ga carbonatites and associated alkaline rocks of the Central-Aldan magnesiocarbonatite province (South Yakutia, Russia). *Mineral. Petrol.* **2019**, *113*, 329–352. [CrossRef]
69. Nikolenko, A.M.; Redina, A.A.; Doroshkevich, A.G.; Prokopyev, I.R.; Ragozin, A.L.; Vladykin, N.V. The origin of magnetite-apatite rocks of Mushgai-Khudag Complex, South Mongolia: Mineral chemistry and studies of melt and fluid inclusions. *Lithos* **2018**, *320–321*, 567–582. [CrossRef]
70. Harlov, D.E.; Förster, H.J.; Nijland, T.G. Fluid induced nucleation of REE-phosphate minerals in apatite: Nature and experiment. Part I. Chlorapatite. *Am. Mineral.* **2002**, *87*, 245–261. [CrossRef]
71. Harlov, D.E.; Förster, H.-J. Fluid-induced nucleation of (Y+REE)-phosphate minerals within apatite: Nature and experiment. Part II. Fluorapatite. *Am. Mineral.* **2003**, *88*, 1209–1229. [CrossRef]
72. Harlov, D.E.; Wirth, R.; Förster, H.J. An experimental study of dissolution–reprecipitation in fluorapatite: Fluid infiltration and the formation of monazite. *Contrib. Mineral. Petrol.* **2005**, *150*, 268–286. [CrossRef]
73. Williams-Jones, A.E.; Migdisov, A.A.; Samson, I.M. Hydrothermal mobilization of the rare earth elements-a tale of "Ceria" and "Yttria". *Elements* **2012**, *8*, 355–360. [CrossRef]
74. Tropper, P.; Manning, C.E.; Harlov, D.E. Solubility of $CePO_4$ monazite and YPO_4 xenotime in H_2O and H_2O–NaCl at 800 °C and 1 GPa: Implications for REE and Y transport during high-grade metamorphism. *Chem. Geol.* **2011**, *282*, 58–66. [CrossRef]
75. Tropper, P.; Manning, C.E.; Harlov, D.E. Experimental determination of $CePO_4$ and YPO_4 solubilities in H_2O–NaF at 800 °C and 1 GPa: Implications for rare earth element transport in high-grade metamorphic fluids. *Geofluids* **2013**, *13*, 372–380. [CrossRef]
76. Broom-Fendley, S.; Styles, M.T.; Appleton, J.D.; Gunn, G.; Wall, F. Evidence for dissolution-reprecipitation of apatite and preferential LREE mobility in carbonatite-derived late-stage hydrothermal processes. *Am. Mineral.* **2016**, *101*, 596–611. [CrossRef]